ENGINEERING TRANSACTIONS • *Engng. Trans.* • **56**, 4, 325–344, 2008
Polish Academy of Sciences • Institute of Fundamental Technological Research

HEAT AND MASS TRANSFER IN MHD FLOW FROM A PERMEABLE SURFACE WITH HEAT GENERATION EFFECTS

M. M. A b d e l k h a l e k

Nuclear Physics Department
Atomic Energy Authority, Nuclear Research Centre
Cairo, Egypt, 13759

The objectives of the present study are to investigate steady two-dimensional laminar flow of a viscous incompressible, electrically conducting and heat-generating fluid, driven by a continuously moving porous plate immersed in a fluid-saturated porous medium, in the presence of a transverse magnetic field. A uniform magnetic field acts perpendicularly to the porous surface which absorbs fluid with a suction velocity. The non-linear partial differential equations governing the problem under consideration have been transformed by a similarity transformation into a system of ordinary differential equations, which is solved numerically by applying a perturbation technique. The effects of material parameters on the velocity and temperature fields across the boundary layer are investigated [28, 29]. A parametric study of all the governing parameters is carried out and representative results are illustrated to reveal a typical tendency of the solutions. Representative results are presented for the velocity temperature distributions as well as the local friction coefficient and the local Nusselt number. Favorable comparisons with the previously published work confirm the correctness of the numerical results.

Key words: heat and mass transfer, magnetohydrodynamics, heat generation, porous media, numerical analysis.

1. Introduction

The study of the dynamics of conducting fluid finds applications in a variety of engineering problems, the ones related to the cooling processes of nuclear reactors, and those related to the connected flow through a porous medium, since the geothermic region gases are electrically conducting and affected by a magnetic field. Recently many authors has been attracted to magnetohydrodynamic convection problems in non-porous medium, (Sparrow and Cess [1]; Riley [2]; Raptis and Singh [3]; Sacheti *et al.* [4]; and Hussein [5]. Some works are available in the subject of MHD convection in porous medium (Kafoussias [6]; Gulab and Mishra [7]; Raptis and Kafousias [8]; Raptis [9]; Takhar and Ram [10] and Abdelkhalek [11–16]). There has been considerable interest in studying flow and heat transfer characteristics of electrically conducting and heat-generating/absorbing fluids (Moalem [17]; Chakrabarti and

Gupta [18]; Vajravelu and Nayfeh [19]; Chiam [20]; Chamkha [21]; Chandran *et al.* [22]; Hadjinicalaou [23]; Chamkha [24], Al–Mudhaf *et al.* [25] and Ramirez–Iraheta *et al.* [26]).

The main objective of this analysis is the investigation of steady two-dimensional laminar flow of a viscous incompressible, electrically conducting and heat generating fluid, driven by a continuously moving porous plate immersed in a fluid-saturated porous medium, in the presence of a transverse magnetic field. A uniform magnetic field acts perpendicularly to the porous surface which absorbs fluid with a suction velocity. A similarity transformation is used to simplify the numerical effort and a numerical solution for the problem is obtained by the perturbation technique [28, 29]. Numerical results are presented concerning the effects of the Hartmann number, Prandtl number, Darcy number, dimensionless heat generation/absorption coefficient and suction injection parameter. Typical results for the velocity and temperature distributions are presented for various governing parameters. Also, the local skin friction coefficients as well as the heat and mass transfer results are illustrated for representative values of the major parameters.

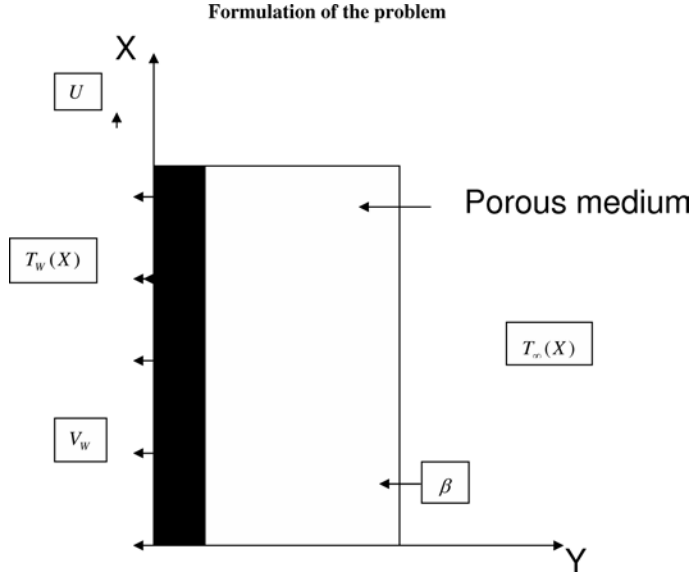

Fig. 1. Physical model and coordinate system.

Consider a two-dimensional steady, laminar, incompressible boundary-layer flow of an electrically conducting and heat-generating fluid, over a porous flat surface embedded in a porous medium, and subjected to a transverse magnetic field (see Fig. 1). It is assumed that there is no applied voltage what implies the absence of an electric field. The transversely applied magnetic field and magnetic

Reynolds number are very small and hence the induced magnetic field is negligible. Viscous and Darcy's resistance terms are taken into account with constant permeability of the porous medium. The MHD term is derived from the order of magnitude analysis of the full Navier–Stokes equations. All thermophysical properties are assumed to be constant. The effects of viscous dissipation, Ohmic heating and Hall currents are neglected. The X-axis is placed along the horizontal plate and Y-axis is perpendicular to it. Let the plate be moving with a constant speed U and at a temperature T_w. Above the plate, the fluid is stationary and is kept at a temperature T_∞. Under the above assumptions, the boundary layer equations governing the flow and heat transfer over an infinite plate can be written as follows [33].

The continuity equation,

$$u_X + v_Y = 0. \tag{1.1}$$

The momentum equation,

$$uu_X + vu_Y = \xi\, u_{YY} - K^{-1}\xi\, u - Cu^2 - \sigma\,\beta^2\rho^{-1}u. \tag{1.2}$$

The energy equation,

$$uT_X + vT_Y = \rho^{-1}C_P^{-1}\left(Q\,(T - T_\infty) + K_e T_{YY}\right), \tag{1.3}$$

where X and Y are the dimensional distances along and normal to the surface, respectively; u and v are the components of dimensional velocities along X and Y directions, respectively; T is the temperature, ρ is the fluid density of the medium, ξ is the kinematic viscosity, C_P is the specific heat at constant pressure, K is the permeability of the porous medium, C is the Forcheimer inertia coefficient, K_e is the effective thermal conductivity, β is the magnetic induction, σ is the fluid electrical conductivity and Q is the heat generation/absorption coefficient. The second term on the right-hand side of the momentum Eq. (1.2) denotes the bulk matrix linear resistance, i.e. the Darcy term and the fourth is the MHD term.

The appropriate boundary conditions for the velocity and temperature fields are given by:

$$\begin{aligned} &Y = 0, \qquad u(X) = U, \qquad v(X) = -v_w(X), \qquad T(X) = T_w, \\ &Y \to \infty, \qquad u(X) = 0, \qquad T(X) = T_\infty, \end{aligned} \tag{1.4}$$

where U is a constant, $v_w(X) > 0$ is the fluid suction at the plate surface, and $v_w(X) < 0$ is the fluid blowing or injection at the wall.

In order to make the results more general in their applicability, the equations are solved in non-dimensional form. For this purpose, the following non-dimensional variables are defined:

$$
\begin{aligned}
&Y = \left(\frac{2\xi\, X}{U}\right)^{0.5} \eta, && u = U\, F'(\eta),\\
&v = \left(\eta\, F' - F\right)\left(\frac{\xi\, U}{2X}\right)^{0.5}, && \theta = \frac{T - T_\infty}{T_w - T_\infty}.
\end{aligned}
\tag{1.5}
$$

With a new set of independent and dependent variables, defined by Eq. (1.5), Eq. (1.1) is identically satisfied, and the partial differential equations (1.2)–(1.3) transform into the ordinary differential equations (1.6)–(1.7).

$$
F''' + FF'' - \left(\left(M + D^{-1}\right) - \alpha_X F'\right) F' = 0, \tag{1.6}
$$

$$
\theta'' + P_r\left(F\,\theta' + \gamma_X\,\theta\right) = 0. \tag{1.7}
$$

Primes denote derivatives with respect to η.

The appropriate flat plate, with the free-convection boundary conditions Eq. (1.4), is also transformed into the applicable form, Eq. (1.8):

$$
\begin{aligned}
&\eta = 0, && F = F_w, && F' = 1, && \theta = 1,\\
&\eta \to \infty, && F' = 0, && \theta = 0,
\end{aligned}
\tag{1.8}
$$

where $M = \sqrt{\dfrac{2\sigma\, x\beta(x)^2}{\rho\, U^2}}$ is the Hartmann number, $D^{-1} = \dfrac{2\xi X}{KU}$ is the inverse Darcy number, $\alpha_X = 2CX$ is the dimensionless inertia coefficient, $P_r = \dfrac{\rho\,\xi\, C_P}{K_e}$ is the Prandtl number, $\gamma_X = \dfrac{2Q\, X}{U\rho\, C_P}$ is the dimensionless heat generation/absorption coefficient, $F_w = -v_w(X)\sqrt{\dfrac{2X}{\xi\, U}}$ is the dimensionless suction/blowing coefficient.

The resulting differential equations contain arbitrary parameters, the Prandtl number, the magnetic field strength and the buoyancy force. Solutions for the resulting semi-infinite domain, nonlinear equations are accomplished with a three the part series method. The employed power series, Eq. (1.9), contains term A that satisfies the boundary conditions and differential equations at infinity, the second term that satisfies the boundary conditions at zero and is the solution to the initial homogeneous differential equation, and additional terms that are

utilized to obtain a better numerical accuracy. This accuracy is limited by the number of terms that will not initiate divergence of the numerical results:

$$F = A + \varepsilon F_1 + \varepsilon^2 F_2 + \varepsilon^3 F_3 + \cdots \tag{1.9}$$

$$\Theta = \varepsilon\theta_1 + \varepsilon^2\theta_2 + \varepsilon^3\theta_3 + \cdots \tag{1.10}$$

which are subject to the boundary conditions which become:

$$\begin{aligned} &\eta = 0, && F_1 = F_w, && F_2 = F_3 = 0, && F_1' = 1, \\ &F_2' = F_3' = 0, && \theta_1 = 1, && \theta_2 = \theta_3 = 0, && \eta \to \infty, \\ &F_n' = 0, && \theta_n = 0, && n = 1, 2, 3. \end{aligned} \tag{1.11}$$

Equation (1.10), the temperature representation, along with Eq. (1.9) and the associated boundary conditions (1.11), contain an undetermined parameter ε which helps in the collection of terms for each set of the resulting linear differential equations. In some problems, it will have a physical meaning which results in a power series of that parameter. Substitution of the series representation into the differential equations and collection of terms with the same powers of ε result in a set of linear differential equations, and the first three sets are:

$$F_1''' + AF_1'' - \left(M + D^{-1}\right) F_1' = 0, \tag{1.12}$$

$$\theta_1'' + P_r A\theta_1' + P_r\gamma_X\theta_1 = 0, \tag{1.13}$$

$$F_2''' + AF_2'' - \left(M + D^{-1}\right) F_2' = \alpha_X F_1'^2 - F_1F_1'', \tag{1.14}$$

$$\theta_2'' + P_r A\theta_2' + P_r\gamma_X\theta_2 = -P_rF_1\theta_1', \tag{1.15}$$

$$F_3''' + AF_3'' - \left(M + D^{-1}\right) F_3' = 2\alpha_X F_1'F_2' - F_1F_2'' - F_2F_1'', \tag{1.16}$$

$$\theta_3'' + P_rK\theta_3' + P_r\gamma_X\theta_3 = -P_rF_1\theta_2' - P_rF_2\theta_1'. \tag{1.17}$$

The solutions to the first three sets, Eqs. (1.18)–(1.23), when substituted into Eqs. (1.9) and (1.10), provide the required representations for F and Θ. The constant A is determined by satisfying the boundary conditions $F(0)$ and is a function of P_r and M.

$$\theta_1 = e^{-a_2\eta}, \tag{1.18}$$

$$F_1 = \left(f_w + a_1^{-1}\right) - a_1^{-1}e^{-a_1\eta}, \tag{1.19}$$

$$\theta_2 = \left(-a_8 + a_7\eta\right) e^{-a_2\eta} + a_8e^{-(a_1+a_2)\eta}, \tag{1.20}$$

$$F_2 = a_6 + (a_5 + a_4\eta)\, e^{-a_1\eta} + a_3 e^{-2a_1\eta}, \tag{1.21}$$

$$\theta_3 = \left(a_{18}\eta + a_{19}\eta^2 - a_{21} - a_{22}\right) e^{-a_2\eta} + (a_{21} + a_{20}\eta)\, e^{-(a_1+a_2)\eta} + a_{22} e^{-(2a_1+a_2)\eta}, \tag{1.22}$$

$$F_3 = -(a_{13} + a_{14} + a_{17}) + \left(a_{17} + a_{15}\eta + a_{16}\eta^2\right) e^{-a_1\eta} + (a_{13} + a_{12}\eta)\, e^{-2a_1\eta} + a_{14} e^{-3a_1\eta}. \tag{1.23}$$

The constants a_i, $i = 1, 2, 3, ..., 22$ are given in the Appendix.

The series for Θ, its first derivative $\Theta'(0)$ – the wall temperature gradient, F' – the velocity profile, and $F''(0)$ – the wall velocity gradient. Knowing the velocity, we can calculate the skin friction and from the temperature field, the rate of heat transfer in terms of the Nusselt number; thus, the skin friction coefficient $C_f R_e^{0.5} = -F''(0)$, and the Nusselt number $\mathrm{Nu} = -R_e^{0.5}\Theta'(0)$, where $R_e = \dfrac{UX}{2\xi}$ is the Reynolds number, $\mu = \dfrac{\xi}{\rho}$ is the dynamic viscosity.

2. Results and discussion

In order to verify the accuracy of our present method, a comparison is made of non-dimensional wall temperature gradient $\Theta'(0)$ with those reported by Jacobi [30], Tsou *et al.* [31], Ali [32] and Chamkha [33] for various values of the Prandtl number P_r. Either, a comparison of non-dimensional wall velocity gradient $F''(0)$ with those reported by Chandran *et al.* [22] and Chamkha [33], for various values of the suction/blowing coefficient F_w. The result of this comparison is given in Tables 1 and 2. The comparisons of all the above cases are found to be in excellent agreement. Sets of representative numerical results are illustrated graphically.

Figures 2 and 3 illustrate variations of different values of magnetic field pa-

Table 1. Comparison of non-dimensional wall temperature gradient ($-\Theta'(0)$) for various values of the Prandtl number.

	$P_r = 0.7$	$P_r = 1.0$	$P_r = 10.0$
Jacobi A.M. [30]	0.3492	0.4438	1.6790
Tsou *et al.* [31]	0.3492	0.4438	1.6804
Ali M. [32]	0.3476	0.4416	1.6713
Chamkha A.J. [33]	0.3524	0.4453	1.6830
Present work	0.35145	0.4468	1.6845

Table 2. Comparison of non dimensional wall velocity gradient ($-F''(0)$) for various values of F_w.

	$F_w = -0.2$	$F_w = -0.1$	$F_w = 0.0$	$F_w = 0.1$	$F_w = 0.2$
Chandran *et al.* [22]	0.5155	0.5700	0.6275	0.6881	0.7515
Chamkha [33]	0.5174	0.5714	0.6288	0.6894	0.753
Present work	0.5168	0.5725	0.62834	0.68864	0.75264

rameter (M) for non-dimensional velocity and non-dimensional distributions of temperature, respectively. Flows were subjected to transverse magnetic fields and wall temperatures that were constant or varied as a fractional power of the distance in the flow direction. General results of these investigations are that the imposed magnetic field decreases the velocity field, wall shear, flow rate and wall heat transfer; also the onset of free convection was retarded while the fluid temperature and the time required for the flow to reach steady state were increased. In addition, considerable influences on the flow and thermal fields can be produced under moderate magnetic field strengths only for liquid metal flows, while the effects of induced magnetic fields and Joule heating are very small. This is illustrated by the reduction of $F'(\eta)$ and growth of $\Theta(\eta)$ as M increases in Figs. 2 and 3, respectively.

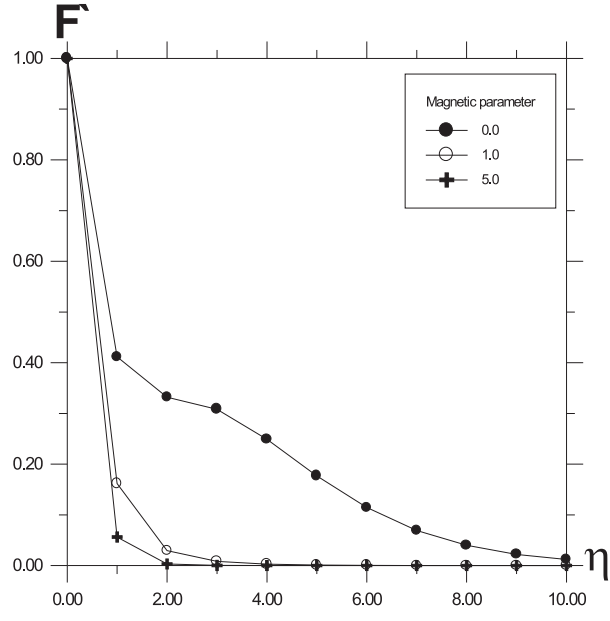

Fig. 2. Variation of velocity profiles F' with η, for $M = 0, 1, 5$, $D^{-1} = .1$, $R_e = 400$, $\alpha_X = .1$, $A = .725$.

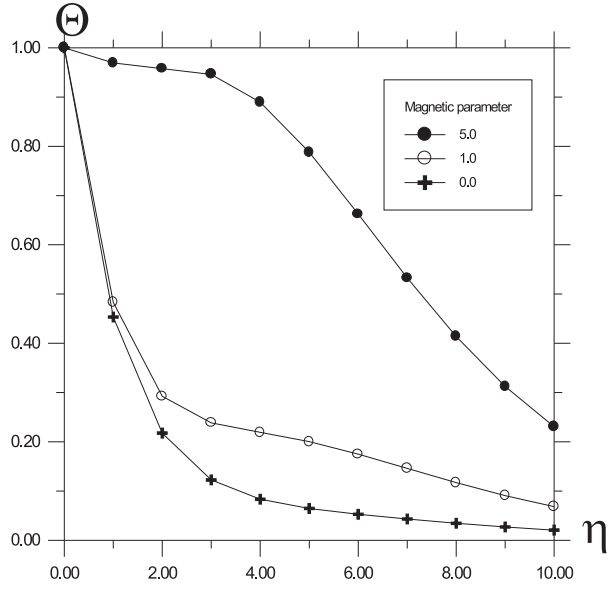

FIG. 3. Variations of temperature profiles Θ with η, for $M = 0, 1, 5$, $D^{-1} = .1$, $R_e = 400$, $\alpha_X = .1$, $A = .725$.

The effect of surface mass transfer F_w on the dimensionless velocity and temperature distributions is displayed in Figs. 4 and 5. The effect of suction consists in making the velocity and temperature distribution more uniform within the boundary layer. Imposition of fluid suction at the surface has a tendency to reduce both the hydrodynamic and thermal thickness of the boundary layer, where viscous effects dominate. This has the effect of reducing both the fluid velocity and temperature above the plate. This follows from the decreases in non-dimensional temperature $\Theta(\eta)$ as the suction/injection parameter F_w increases, as shown in Figs. 4 and 5.

Figures 6 and 7 show the changes in the fluid tangential and normal non-dimensional velocity and non-dimensional temperature, as the inverse Darcy number (D^{-1}) and the non-dimensional porous medium inertia coefficient are altered, respectively. The parameter (D^{-1}) represent resistance to the flow since they restrict the motion of the fluid along the plate. Therefore they have the same effect as the magnetic parameter M, they are decreasing the fluid velocity and increasing its temperature as shown in the figures. Figures 8 and 9 show the effect of non-dimensional porous medium inertia coefficient (α_x) on the non-dimensional velocity and non-dimensional temperature profiles. The parameter α_x represents resistance to flow since it reduces the motion of the fluid along the plate. Therefore they have the same effect as the magnetic parameter M, they are decreasing the fluid velocity and increasing its temperature, as shown in the figures.

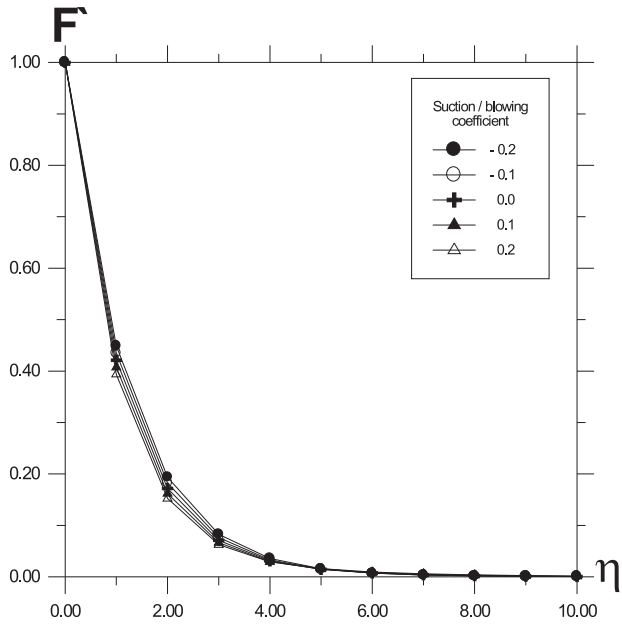

FIG. 4. Variation of velocity profiles F' with η, for $f_w = -.2, -.1, 0, .1, .2$, $D^{-1} = .1$, $R_e = 400$, $\alpha_X = .1$, $A = .725$.

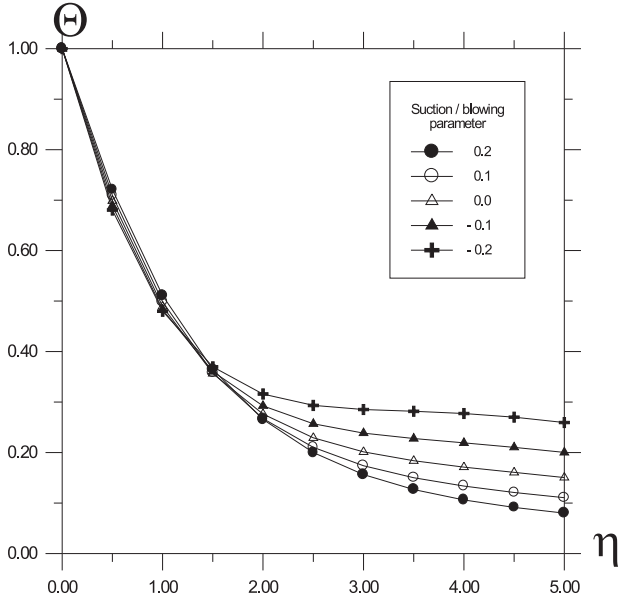

FIG. 5. Variations of temperature profiles Θ with η, for $f_w = -.2, -.1, 0, .1, .2$, $D^{-1} = .1$, $R_e = 400$, $\alpha_X = .1$, $A = .725$.

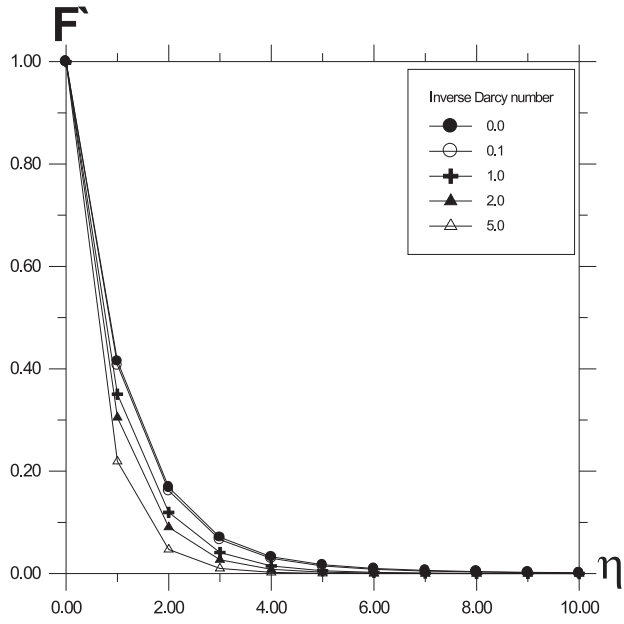

FIG. 6. Variation of velocity profiles F' with η, for $D^{-1} = 0, .1, 1, 2, 5$, $R_e = 400$, $\alpha_X = .1$, $M = 1$, $A = .725$.

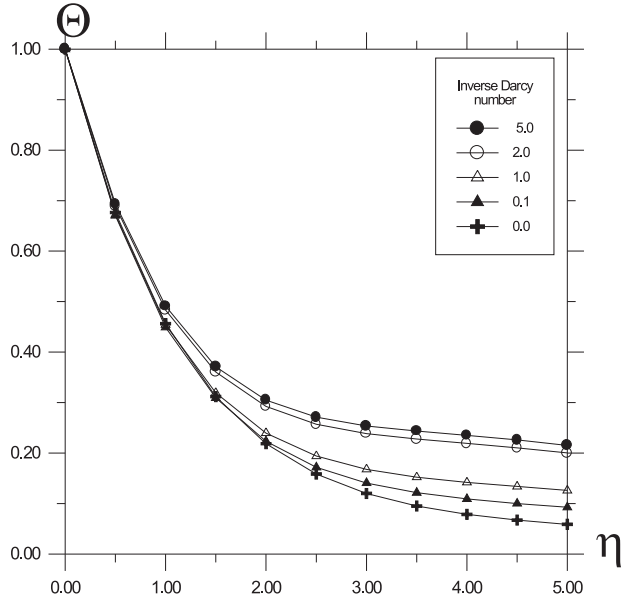

FIG. 7. Variations of temperature profiles Θ with η, for $D^{-1} = 0, .1, 1, 2, 5$, $R_e = 400$, $\alpha_X = .1$, $M = 1$, $A = .725$.

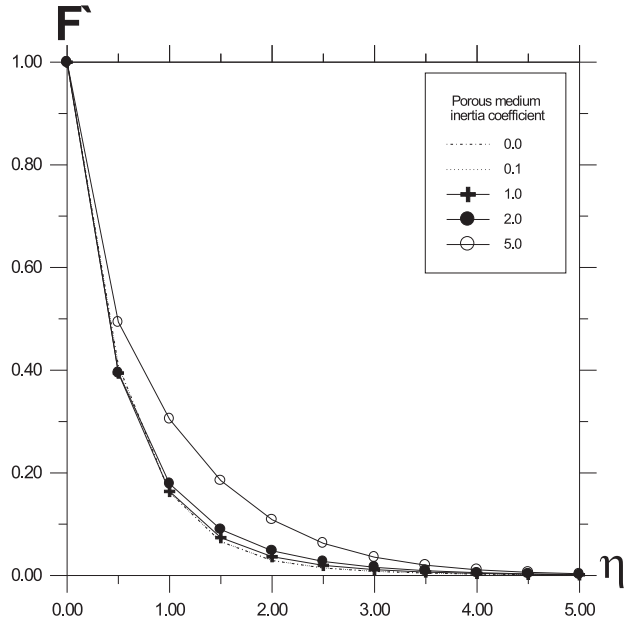

FIG. 8. Variation of velocity profiles F' with η, for $\alpha_X = 0, .1, 1, 2, 5$, $M = 1$, $D^{-1} = .1$, $\gamma_X = 0$, $f_w = .1$.

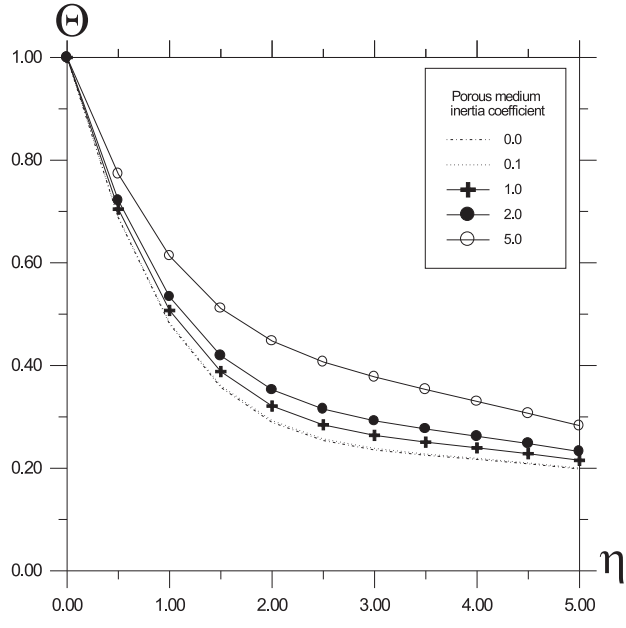

FIG. 9. Variations of temperature profiles Θ with η, for $\alpha_X = 0, .1, 1, 2, 5$, $M = 1$, $D^{-1} = .1$, $\gamma_X = 0$, $f_w = .1$.

Figure 10 presents the influence of various values of Prandtl number on the non-dimensional temperature profile. Increasing the Prandtl number reduces the thermal boundary layer along the plate. This yields a reduction in the fluid temperature. The reason of this effect is that higher Prandtl number implies more viscous fluid which increases the boundary layer thickness, and this causes reduction in the shear stress. The effects of inverse Darcy number D^{-1} on the non-dimensional surface velocity gradient is shown in Fig. 11. The presence of a porous medium in the flow presents resistance to flow, thus, slowing the flow and increasing the pressure reduction across it. Therefore, as the inverse Darcy number D^{-1} increases, the resistance due to the porous medium increases and the surface velocity gradient increases. It is seen from the figure that the skin friction increases monotonically with increasing parameter M. Figure 12 illustrates the change in the value of non-dimensional surface temperature $(-\Theta'(0))$ as a result of changing both the Hartmann parameter M and inverse Darcy number D^{-1}. It is seen from the figure that the non-dimensional surface temperature $(-\Theta'(0))$ decreases monotonically with increasing parameter M and decreases with increasing D^{-1}. The reason for this is that the presence of a porous medium D^{-1} causes higher restriction to the fluid flow, which in turn slows its motion. As a result of this, the Nusselt number at the plate surface decreases. The variations of various values of the dimensionless suction/blowing coefficient on the

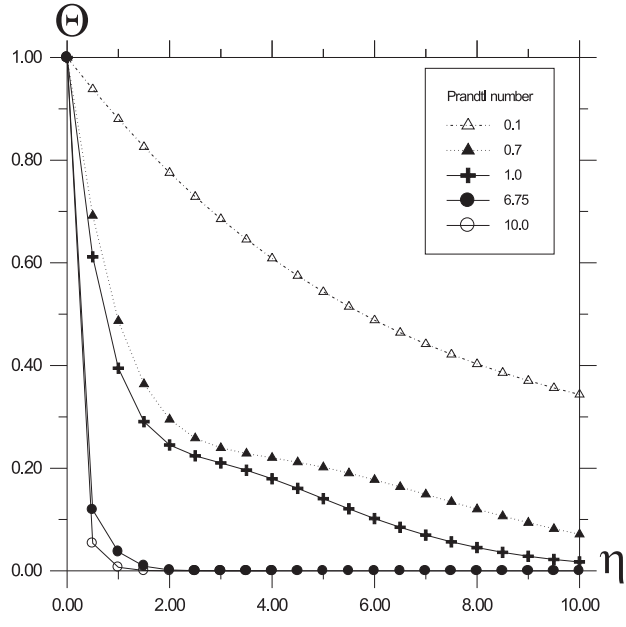

FIG. 10. Variation of temperature profiles Θ with η, for $P_r = -.1, -.7, 1, 6.75, 10$, $\gamma_X = 0$, $f_w = .1$, $R_e = 400$, $A = .725$, $M = 1$, $D^{-1} = .1$.

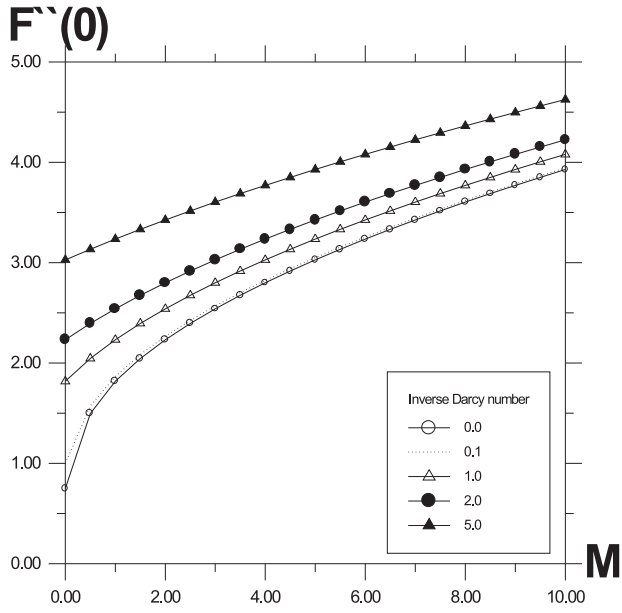

FIG. 11. Variation of wall velocity gradient profiles F'' with M, for $D^{-1} = 0, .1, 1, 2, 5$, $R_e = 400$, $A = 1.25$, $\eta = 1$, $\alpha_X = .1$, $\gamma_X = 0$, $f_w = .1$.

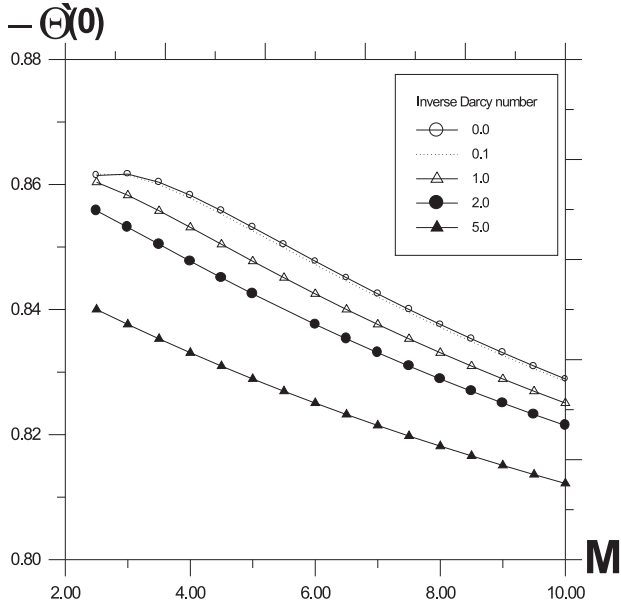

FIG. 12. Variation of wall temperature gradient profiles Θ' with M, for $D^{-1} = 0, .1, 1, 2, 5$, $R_e = 400$, $A = .875$, $\eta = 1$, $\alpha_X = .1$, $\gamma_X = 0$, $f_w = .1$.

non-dimensional surface velocity gradient profiles F'' is shown in Fig. 13. It is seen from the figure that, as expected, the non-dimensional surface velocity gradient profiles F'' increase monotonically with increasing magnetic parameter M. Blowing decreases the wall shear stress both in free and forced convection flows. Suction decreases the wall shear stress in the free convection flow but increases it in forced convection flow. This is clear from the figure. LIEN *et al.* [34] reported a similar result for the isothermal wall temperature condition for free convection flows.

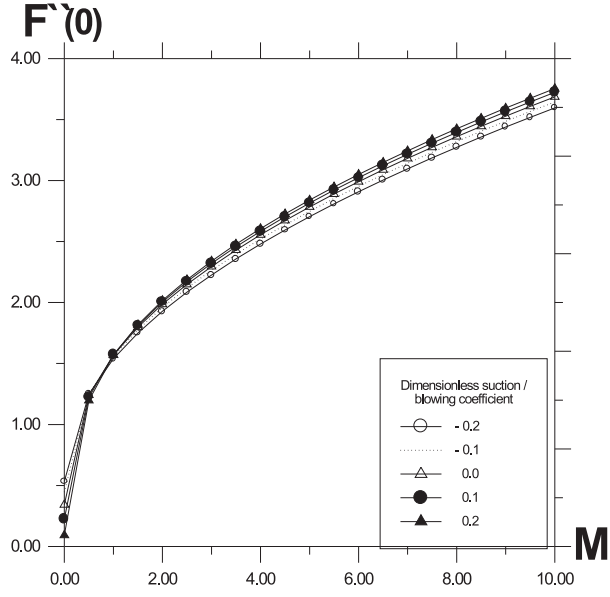

FIG. 13. Variation of wall velocity gradient profiles with M, for $f_w = -.2, -.1, 0, .1, .2$, $R_e = 400$, $A = .875$, $\eta = 1$, $\alpha_X = .1$, $\gamma_X = 0$, $P_r = .7$, $D^{-1} = .1$.

The effects of suction/blowing coefficient F_w on the non-dimensional wall temperature gradient is presented in Fig. 14. The suction makes the temperature distribution more uniform within the boundary layer and decreases the thermal boundary layer thickness. The non-dimensional wall temperature gradient increases as the suction/blowing parameter F_w increases. It is seen from the figure that the non-dimensional wall temperature gradient profiles increase monotonically with increasing parameter M. Figure 15 illustrates the change in the values of non-dimensional wall temperature gradient with various values of the dimensionless heat generation/absorption coefficient Q and Prandtl number P_r. Increasing the value of P_r reduces the thermal boundary layer along the plate. This reduces the fluid temperature at every point above the plate surface and increases the dimensional wall temperature gradient. The non-dimensional wall temperature gradient increases as the Prandtl number P_r increases. The reason for this

trend is that higher Prandtl number implies more viscous fluid which increases the boundary layer thickness and this causes reduction in the shear stress.

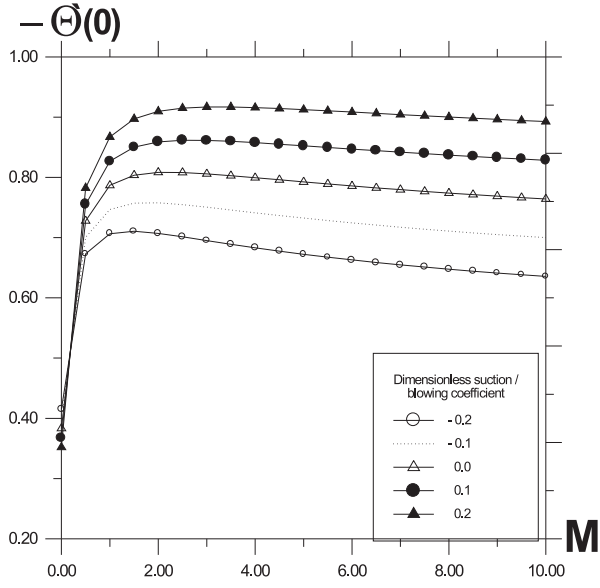

FIG. 14. Variation of wall temperature gradient profiles Θ' with M, for $f_w = -.2, -.1, 0, .1, .2$, $R_e = 400$, $A = .875$, $\eta = 1$, $\alpha_X = .1$, $\gamma_X = 0$, $P_r = .7$, $D^{-1} = .1$.

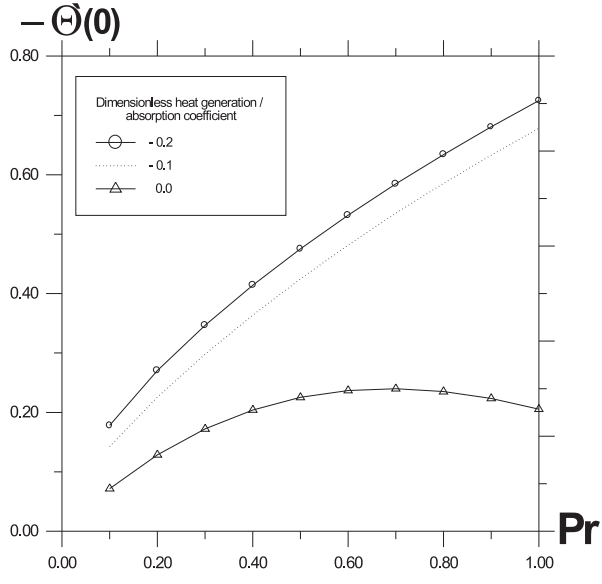

FIG. 15. Variation of wall temperature gradient profiles Θ' with P_r, for $Q = -.2, -.1, 0$, $R_e = 400$, $A = 1.75$, $\eta = 1$, $\alpha_X = .1$, $\gamma_X = 0$, $M = 1$, $D^{-1} = .1$.

3. Conclusions

The problem of steady, laminar, simultaneous heat and mass transfer by natural convection boundary layer flow of an electrically-conducting and heat-generating fluid, driven by a continuously moving porous plate immersed in a fluid saturated porous medium in the presence of a transverse magnetic field was considered. The resulting transformed governing equations are solved numerically by a perturbation technique. The results are presented for the major parameters including the magnetic parameter, the Prandtl number, Darcy number, the dimensionless heat generation/absorption coefficient and the dimensionless suction/blowing coefficient. A systematic study on the effects of the various parameters on flow, heat and mass transfer characteristics is carried out. The particular conclusions drawn from this study can be listed as follows:

1. In the presence of a magnetic field, the velocity is found to be decreased, associated with a reduction in the velocity gradient at the wall, and thus the local skin-friction coefficient decreases. Also, the applied magnetic field tends to decrease the wall temperature gradient which yields a decrease in the local Nusselt number.
2. The effect of energy generation, varying in space and with local temperature, is to heat the fluid and increase the velocities inside the boundary layer and consequently, to decrease the heat transfer rates and increase the skin friction. On the contrary, the effect of energy absorption terms either space or temperature-dependent, is to cool the fluid and consequently, to increase the heat transfer rates. The mean skin friction increases with increasing of the suction parameter and decreases as the Prandtl number increases. The mean rate of heat transfer increases as the suction parameter or the Prandtl number increase, but decreases as the space or temperature-dependent heat generation term increases.
3. To increase the buoyancy ratio is to increase the local skin friction. On the other hand, increasing the buoyancy may increase or decrease the local Nusselt number, depending upon the competition between the impacts of viscous dissipation and the buoyancy ratio.
4. The local Nusselt number can be increased by increasing the values of the Prandtl number and the wall temperature. Heat is found to be transferred from the fluid to the plate (which is indicated by a negative Nusselt number) at a negative value.
5. As compared to an impermeable surface, the local skin-friction, the local Nusselt number will increase when suction is present at the permeable wall, where as the opposite trend is true for the case when the wall is subjected to injection of fluid.

Appendix

$$a_1 = \frac{A + \sqrt{A^2 + 4\left(M + D^{-1}\right)}}{2},$$

$$a_2 = \frac{P_r A + \sqrt{P_r^2 A^2 - 4P_r\gamma_X}}{2},$$

$$a_3 = \frac{\left(\alpha_X - 1\right)}{-2a_1\left(4a_1^2 - 2a_1 A - \left(M + D^{-1}\right)\right)},$$

$$a_4 = \frac{-a_1\left(F_w + a_1^{-1}\right)}{\left[-3a_1^2 + 2Aa_1 + \left(M + D^{-1}\right)\right]},$$

$$a_5 = \frac{-2a_1a_3 + a_4}{a_1},$$

$$a_6 = -a_5 - a_3,$$

$$a_7 = \frac{\left(F_w + a_1^{-1}\right)a_2P_r}{P_rA - 2a_2},$$

$$a_8 = \frac{-a_2P_r}{a_1\left(\left(a_1 + a_2\right)\left(\left(a_1 + a_2\right) - P_rA\right) + P_r\gamma_X\right)},$$

$$a_9 = \left(\left(F_w + a_1^{-1}\right)\left(a_1^2a_5 - 2a_1a_4\right)\right),$$

$$a_{10} = \left(\left(F_w + a_1^{-1}\right)4a_1^2a_3 - a_1a_5 + 2a_4\right),$$

$$a_{11} = \left(F_w + a_1^{-1}\right)a_1^2a_4,$$

$$a_{12} = \frac{2a_1a_4\left(1 - \alpha_X\right)}{-2a_1\left(4a_1^2 - 2Aa_1 - \left(M + D^{-1}\right)\right)},$$

$$a_{13} = \frac{\left(2\alpha_X\left(-a_1a_5 + a_4\right) - a_{10} + a_1a_5\right) - a_{12}\left(12a_1^2 - 4Aa_1 - \left(M + D^{-1}\right)\right)}{-2a_1\left(4a_1^2 - 2Aa_1 - \left(M + D^{-1}\right)\right)},$$

$$a_{14} = \frac{a_1a_3\left(5 - 4\alpha_X\right)}{-3a_1\left(9a_1^2 - 3a_1A - \left(M + D^{-1}\right)\right)},$$

$$a_{15}=\frac{(a_1a_6-a_9)\left(6a_1^2-4Aa_1-2(M+D^{-1})\right)+a_{11}(2A-6a_1)}{\left(3a_1^2-2Aa_1-(M+D^{-1})\right)\left(6a_1^2-4Aa_1-2(M+D^{-1})\right)-a_1(2A-6a_1)\left(-a_1^2+Aa_1-(M+D^{-1})\right)},$$

$$a_{16}=\frac{-a_{11}\left(3a_1^2-2Aa_1-(M+D^{-1})\right)-a_1\left(-a_1^2+Aa_1+(M+D^{-1})\right)(a_1a_6-a_9)}{\left(3a_1^2-2Aa_1-(M+D^{-1})\right)\left(6a_1^2-4Aa_1-2(M+D^{-1})\right)-a_1(2A-6a_1)\left(-a_1^2+Aa_1-(M+D^{-1})\right)},$$

$$a_{17}=a_1^{-1}\left(a_{12}-2a_1a_{13}-3a_1a_{14}+a_{15}\right),$$

$$a_{18}=\frac{\left(-P_r\left(F_w+a_1^{-1}\right)(a_7+a_2a_8)+a_2a_6P_r\right)(2P_rA-4a_2)-2P_ra_2a_7\left(F_w+a_1^{-1}\right)}{(P_rA-2a_2)(2P_rA-4a_2)-2\left(a_2^2-P_rAa_2+P_rQ_X\right)},$$

$$a_{19}=\frac{(P_rA-2a_2)\left(P_r(F_w+a_1^{-1})a_2a_7\right)-\left(a_2^2-P_rAa_2+P_r\gamma_X\right)\left(-P_r(F_w+a_1^{-1})(a_2a_8+a_7)+a_2a_6P_r\right)}{(P_rA-2a_2)(2P_rA-4a_2)-2\left(a_2^2-P_rAa_2+P_r\gamma_X\right)},$$

$$a_{20}=\frac{-a_2a_7P_r}{a_1\left((a_1+a_2)\left((a_1+a_2)-P_rA\right)+P_r\gamma_X\right)},$$

$$a_{21}=\frac{\left(P_r\left(F+a_1^{-1}\right)a_8(a_1+a_2)+P_ra_1^{-1}(a_7+a_2a_8)-a_{20}\left(P_rA-2(a_1+a_2)\right)\right)}{\left((a_1+a_2)\left((a_1+a_2)-P_rA\right)+P_r\gamma_X\right)},$$

$$a_{22}=\frac{-a_8P_r(a_1+a_2)}{a_1\left((2a_1+a_2)\left((2a_1+a_2)-P_rA\right)+P\gamma_X\right)}.$$

Reynolds number = Inertia force/Viscous force = $R_e=\rho\nu L/\mu$; the higher is the Reynolds number, the greater will be the relative contribution of the inertia effect. The smaller is the Reynolds number, the greater will be the relative magnitude of the viscous stress.

The Hartmann number $R_h=(R_eR_HR_\sigma)^{0.5}$ is the ratio of the magnetic force to the viscous force and it was introduced by Hartmann in order to describe his experiments with viscous magnetohydrodynamic channel flow; the magnetic number $R_m=(R_HR_\sigma)^{0.5}$ is the ratio of the magnetic force to the inertial force, and when R_σ is very small, R_m is also used to measure the electromagnetic effects on the flow.

Prandtl number $P_r=\mu C_P/K=\nu/\alpha$ it is the ratio of kinematic viscosity to thermal diffusivity. It takes into account three physical properties of the fluid at a time. It is the ratio of two constants in molecular transportation. Symbol ν denotes the impulse transport through molecular friction, where α is the heat energy transport by conduction. It physically represents the relative speed at which momentum and energy are propagated through a fluid.

Nusselt number $\mathrm{Nu} = hL/K$, it is a dimensionless heat transfer coefficient, which equals the ratio of the heat transfer rate q to the rate at which heat would be conducted within the fluid under a temperature gradient $\Delta\theta/L$. It can also be defined as the ratio of heat flow rate by convection under unit temperature gradient through a stationary thickness of L meter.

Darcy's model. During the last century, the researchers have derived generalized forms of the Darcy equation using either deterministic or statistical models. The well-known original form of the equation has been rewritten as: $u = -\dfrac{K}{\mu}.\nabla P$ for an isotropic medium, where K is the so-called intrinsic permeability, and ∇P is the pressure gradient. Although Darcy's law can describe the flow through many naturall occurring porous media, it is not valid for all types of situations. In fact, defined for a porous medium, the Reynolds number is based on permeability of the porous medium as $\mathrm{Re}_K \geq 1$. The Darcy number was based on the permeability of the porous medium (K).

Acknowledgments

Appreciation is extended to the Referees for their constructive and helpful comments and suggestions. These led to improvements in the revised paper.

References

1. E. M. Sparrow and R. D. Cess, Int. J. Heat Mass Transfer, **3**, 267, 1961.
2. N. Riley, J. Fluid Mech., **18**, 577, 1964.
3. A. Raptis and A. K. Singh, Int. Comm. Heat Mass Transfer, **10**, 313, 1983.
4. N. C. Sacheti, P. Chamdran and A. K. Singh, Int. Comm. Heat Mass Transfer, **21**, 131, 1994.
5. M. A. Hossain, Int. J. Heat Mass Transfer, **35**, 3485, 1992.
6. N. G. Kafoussias, Mech. Res. Commun., **19**, 89, 1992.
7. R. Gulab and R. Mishra, Indian J. Pure Appl. Math., **8**, 637, 1977.
8. A. Raptis and N. Kafousias, Energy Research, **6**, 241, 1982.
9. A. A. Raptis, Energy Research, **10**, 97, 1986.
10. H. S. Takhar and P. C. Ram, Int. Comm. Heat Mass Transfer, **21**, 371, 1994.
11. M. M. Abdelkhalek, International Communications in Heat and Mass Transfer, **33**, 249, 2006.
12. M. M. Abdelkhalek, Arab J. of Nucl. Sci. and Applications, **36**, 2, 189, 2003.
13. M. M. Abdelkhalek, Indian J. Phys., **80**, 6, 625–635, 2006.

14. M. M. Abdelkhalek, Arab J. of Nucl. Sci. and Applications, **36**, 3, 243, 2003.

15. M. M. Abdelkhalek, CAMES, **14**, 3, 471–485, 2007.

16. M. M. Abdelkhalek, Egyptian J. of Physics, **34**, 3, 2003.

17. D. Moalem, Int. J. Heat Mass Transfer, **19**, 529, 1976.

18. A. Chakrabarti and A. S. Gupta, Q. Appl. Math., **37**, 73, 1979.

19. K. Vajravelu and J. Nayfeh, Int. Commun. Heat Mass Transfer, **19**, 701, 1992.

20. T. C. Chiam, Int. J. Engng. Sci., **33**, 429, 1995.

21. A. J. Chamkha, Int. Commun. Heat Mass Transfer, **23**, 875, 1996.

22. P. Chandran, N. C. Sacheti and A. K. Singh, Int. Commun. Heat Mass Transfer, **23**, 889, 1996.

23. K. Vajravelu and A. Hadjinicalaou, Int. J. Engrg. Sci., **35**, 1237, 1997.

24. A. J. Chamkha, Int. J. of Heat and Fluid Flow, **20**, 84, 1999.

25. Ali Al-Mudhaf and Ali J. Chamkha, Heat Mass Transfer, **42**, 112, 2005.

26. O. A. Ramirez–Iraheta, H. M. Soliman and S. J. Ormiston, Heat Mass Transfer, **42**, 398, 2006.

27. Md. Anwar Hussain and D. A. S. Rees, Heat Mass Transfer, **41**, 367, 2005.

28. A. Aziz, T. Y. Na, *Perturbation Methods in Heat Transfer*, Springer-Verlag, Berlin, 1–184, 1984.

29. R. Kenneth Cramer, Shih-I Pai, *Magnetofluid Dynamics for Engineers and Applied Physicists*, McGraw-Hill Book Company, New York, 164–171, 1973.

30. A. M. Jacobi, J. Heat Transfer, **115**, 1058, 1993.

31. F. K. Tsou, E. M. Sparrow and R.J. Goldstein, Int. J. Heat Mass Transfer, **10**, 219, 1967.

32. M. Ali, Int. J. Heat and Fluid Flow, **16**, 280, 1995.

33. A. J. Chamkha, Int. Comm. Heat Mass Transfer, **24**, 6, 815, 1997.

34. F. S. Lien and C. K. Chen, Trans. ASME, **108**, 398, 1986.

Received October 04, 2007; revised version January 24, 2008.